CHEMISTRY
A European Journal

A Journal of
ChemPubSoc Europe

Accepted Article

Title: Heptazine: A new electron deficient fluorescent core for discotic liquid crystals

Authors: Santanu Kumar Pal, Indu Bala, Harpreet Singh, venugopala rao battula, santosh prasad Gupta, joydip de, Sunil Kumar, and Kamalakannan Kailasam

To be cited as: *Chem. Eur. J.* 10.1002/chem.201703364

Link to VoR: http://dx.doi.org/10.1002/chem.201703364

Supported by
ACES

WILEY-VCH

Heptazine: A new electron deficient fluorescent core for discotic liquid crystals

Indu Bala,[a] Harpreet Singh,[a] Venugopala Rao Battula,[b] Santosh Prasad Gupta,[a] Joydip De,[a] Sunil Kumar,[b] Kamalakannan Kailasam*[b] and Santanu Kumar Pal*[a]

Abstract: Room temperature discotic liquid crystals based on heptazine, a novel electron deficient central core, are reported and their mesomorphic behavior investigated for the first time. Supramolecular assembly of these derivatives in their mesophase were confirmed by their X-ray scattering results. They are strong blue light emitters when fabricated into solid thin films while in solution state, they are weakly emissive or non-emissive. The band gap is found to be low in these class of compounds. Formation of room temperature mesophases, low band gap behaviour and strong blue-light emitters in the solid state making them promising candidates for various optoelectronic applications.

There is a considerable demand of discotic liquid crystals (DLCs) in organic electronics due to their tendency to self-assemble into columnar superstructures with one-dimensional charge carrier migration properties.[1,2] In literature, DLCs with electron-rich cores are numerous, while a few examples of electron deficient systems are known.[3] Such electron deficient discotic molecules with low band gap are potential candidates as excellent organic semiconductors for both positive and negative charge transport materials making them highly promising from device point of view.[4] Further, the charge transport and luminescent properties in this kind of materials can be enhanced by inclusion of an *N*-heterocycle core suitable for applications in electro-optical devices.[4] Moreover, Nitrogen containing polycyclic aromatic core is particularly advantageous as their electronic properties can be tuned from *p*-type to *n*-type (on exchanging the *sp*^{2}-carbon atoms by N atoms) without modifying the overall structure.

In recent years, there has been ever increasing interest in the field of *N*-heterocyclic based discotic materials to the realization of new classes of organic semiconductors.[5-7] In particular, heptazine, since its discovery, have been explored widely as a metal-free catalyst,[8] photo-catalyst for H_2 formation from water splitting,[9] as smart material for potential applications in OLEDs[10] and so on. In addition, heptazine (C_6N_7) possesses a disc-shaped core and although its derivatives have the potential for advanced materials in devices, it has not yet been explored in the field of DLCs. If the intriguing thermal,[11] optical[12-14] and electronic properties[15a] of heptazine are combined with the self-organization features of LCs it will definitely improve their usability in devices. This will also open a new field based on heptazine discotics (an extended version of triazine systems) that might overcome the physical and chemical properties of the equivalent *s*-triazine system due to its larger core.[15b-c]

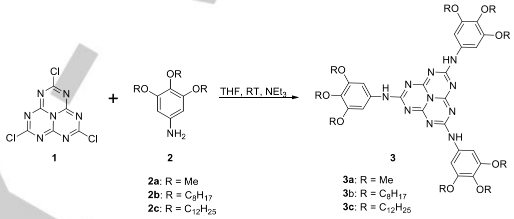

Scheme 1. Synthesis of 3, 4, 5-trialkoxyphenylamine substituted heptazine derivatives.

In this communication, we describe the synthesis and characterization of disc-shaped molecules **3a-c** consisting of a heptazine core attached to which are three tri-alkoxy substituted benzene derivatives *via* amino linkage (Scheme 1). A precursor material heptazine (cyameluric) chloride ($C_6N_7Cl_3$) **1** was reacted with 3,4,5-trialkoxyphenylamine **2** in presence of NEt_3 as a base in THF at room temperature to get the desired product **3**. Compound **1** is sensitive towards hydrolysis and therefore, the reaction was carried out under extremely inert conditions in glove box. The structures of all compounds were characterized using ^{1}H, ^{13}C NMR, IR spectra, HRMS and elemental analysis (Fig. S1-S10, ESI).

Three heptazine derivatives **3a**-**c** were synthesized and their thermal behavior was investigated using a combination of POM, and DSC (Fig. 1 & S12, ESI). Interestingly, compound **3b** and **3c** with peripheral chain lengths *R* = -C_8H_{17} and *R* = -$C_{12}H_{25}$, respectively, were found to be mesomorphic. The compound **3b** with shorter alkyl chain length exhibits smectic (Sm) phase while, **3c** with longer chain length exhibits columnar hexagonal mesophase (Col$_h$) which are well supported by their POM and X-ray diffraction studies (*vide infra*). This behavior is unusual but has been observed in tetraphenylenes system where compounds with lower peripheral alkyl chain length shows smectic behavior while the higher ones self-assembles into columnar structures.[16a] The compound **3a** with R = -Me was synthesized as a model compound and found to be crystalline in nature.

Under POM, compound **3c** exhibits room temperature mesophase. On heating, it starts clearing at 98 °C (ΔH = 5.8 kJ

---

[a] Ms. I. Bala, Mr. H. Singh, Dr. S. P. Gupta, Mr. J. De and Dr. S. K. Pal*
Department of Chemical Sciences
Indian Institute of Science Education and Research (IISER) Mohali
Sector-81, Knowledge city, Manauli-140306, India
E-mail: skpal@iisermohali.ac.in, santanupal.20@gmail.com
[b] Mr. V. R. Battula, Dr. S. Kumar and Dr. K. Kailasam*
Institute of Nano Science and Technology (INST), Sector-64, Phase 10, Mohali 160062, India.
E-Mail: kamal@inst.ac.in

Supporting information for this article is given via a link at the end of the document.

10.1002/chem.201703364

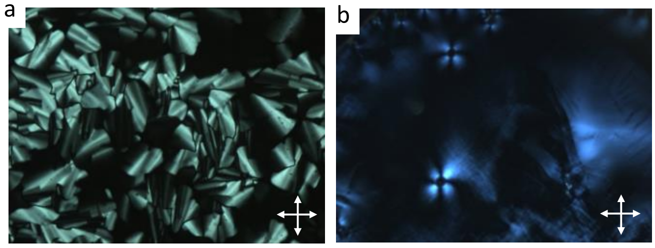

Figure 1. POM images (a) columnar textures of compound **3c** at 80 °C, observed on cooling from the isotropic liquid (b) Orthogonal isogyre textures of compound **3b** at 60 °C, observed on pressing the homeotropically aligned areas develops on the glass slide when cooled from the isotropic liquid, (magnification X 500, crossed polariser).

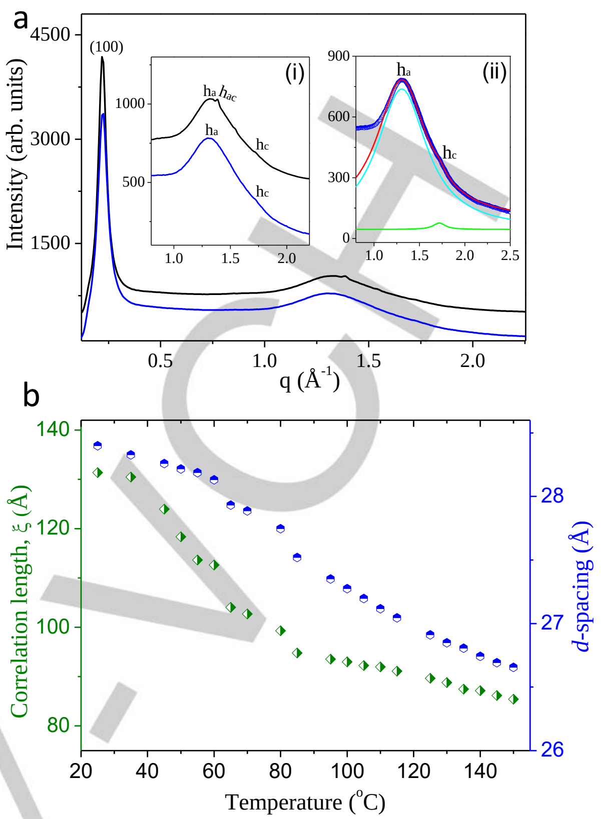

Figure 2. (a) X-ray diffraction pattern of Sm phase of compound **3b** at 25 °C (black colored) and 60 °C (blue colored), Inset shows (i) zoomed area of wide angle regime at 25 °C (black colored) and 60 °C (blue colored) (ii) deconvolution of the wide angle peak at 60 °C, the curve with half-filled diamond in blue color represents the wide angle data. The curves in the cyan and green colors correspond to fluid chain-chain and heptazine core-core (face to face) correlations, respectively. And curve in the red color is the sum of the cyan and green color curve. h_a - fluid chain-chain separations, h_{ac} - crystallize chain-chain separation and h_c – heptazine core-core (face to face wise) separation. (d) Variation of correlation length (ξ) and d-spacing corresponding to the (100) peak with temperature for **3b**.

mol^{-1}) to the isotropic phase as observed from DSC (Fig. S12, ESI). During cooling, the phase appears at 96 °C which remains stable down to room temperature. The texture obtained on cooling at 80 °C from the isotropic phase is shown in Fig. 1a. However, below 45 °C, it exhibits glassy nature (Fig. S11b).

Compound **3b** also exhibits mesophase at room temperature and the phase is mostly homeotropically aligned (Fig. S11c). The compound goes to isotropic at 149 °C (*ΔH* = 4.6 kJ mol^{-1}) which on cooling reappears at 143 °C. The occurrence of orthogonal isogyre textures (on pressing the top of glass slide), as shown in Fig. 1b, indicate the formation of Sm phase.[16b]

Next, Small and wide angle X-ray (SAXS/WAXS) experiments were performed to examine the quantitative details of mesophase behavior of compound **3b** and **3c**. The diffraction pattern of compound **3b** at 60 °C exhibits one sharp peak in the small angle region of spacing 28.13 Å (Fig. 2a). However, in the wide angle regime, one halo peak (h_a) of spacing 4.80 Å with one additional weak peak (h_c) of spacing 3.65 Å were found which is further confirmed by the de-convolution of the wide angle peak as shown in the Fig. 2a (inset (ii)). The diffraction pattern also reinforced the formation of Sm phase. The small angle peak indexed to be (100) and correspond to the layer spacing (*d*). Further, h_a and h_c peaks of the wide angle region reflect the fluid alkyl chain-chain and heptazine core-core (side to side) separations, respectively. The correlation length corresponding to the (100) peak is found to be about 112 Å which correspond to ~ 4 number of correlated layers. The diffraction pattern in the temperature range 45 °C to 150 °C is similar to that of at 60 °C (Fig. S13, ESI). However below 45 °C, the small angle peak (correspond to (100)) is found to be similar to that of at 60 °C with relatively higher *d*-spacings and correlation length value (Fig. 2b). But the wide angle exhibits a narrow peak (h_{ac}) of spacing 4.5 Å in addition to h_a (4.76 Å) and h_c (3.64 Å) peaks (Fig. 2a (inset (i)) & S13, ESI). The h_{ac} peak appears due to crystallize chain-chain correlation and reflect the less fluid behavior at lower temperature. Further, the *d*-spacing [(100) peak] value and corresponding correlation length is found to be decreasing with increasing the temperature (Fig. 2b).

The X-ray diffraction pattern of compound **3c** at 90 °C showed four peaks in the small angle region (Fig. 3a). The corresponding d-spacing are found to be 32.07 Å, 18.54 Å, 16.02 Å and 12.21 Å and they are in ratios $\frac{1}{1}:\frac{1}{\sqrt{3}}:\frac{1}{2}:\frac{1}{\sqrt{7}}$ confirming, the occurrence of 2D hexagonal phase ((Fig. 3a (inset (i)).

According to the ratios, the observed four peaks were assigned to the reflection of the (10), (11), (20) and (21) planes, respectively (Table S1, ESI). In-addition, one broad peak is present in the wide angle region which is found to be the convolution of two peaks corresponding to h_a and h_c peaks of spacing 4.97 Å and 3.76 Å, respectively (Fig. 3a (inset (ii)). Based on the results, the LC phase is best described as the columnar hexagonal (Col$_h$) phase. The corresponding 2D X-ray diffractogram reflects the crescent-moon pattern (Figure 3c,d). The reciprocal lattice vectors *a** and *b** are found to be along the equator and *c** is along the meridian. The corresponding 2D electron density map is shown in the Fig. 3e (see ESI for details). The lattice parameter, *a,* (column- column separation) is calculated by using the relation: $a = \frac{2d_{10}}{\sqrt{3}}$, where d_{10} is the spacing corresponding to (10) peak. The value of the calculated lattice parameter, *a* is found to be 37.04 Å. The h_c peak set the value of the lattice parameter, *c* (distance between heptazine discs within the column) to 3.76 Å representative of π-π stacking of disc in the column. The calculated value of *n* (number of molecule per unit fluid cell of hexagonal lattice) at 90 °C is found to be 1.28 (see ESI) suggesting the formation of hexagonal phase in a monomeric manner but with a significant volume of inter-digitations of alkyl chains.

Further, the observed diffraction pattern in the temperature range 25 °C to 98 °C is very similar to that of at 90 °C (Fig. S14, ESI).

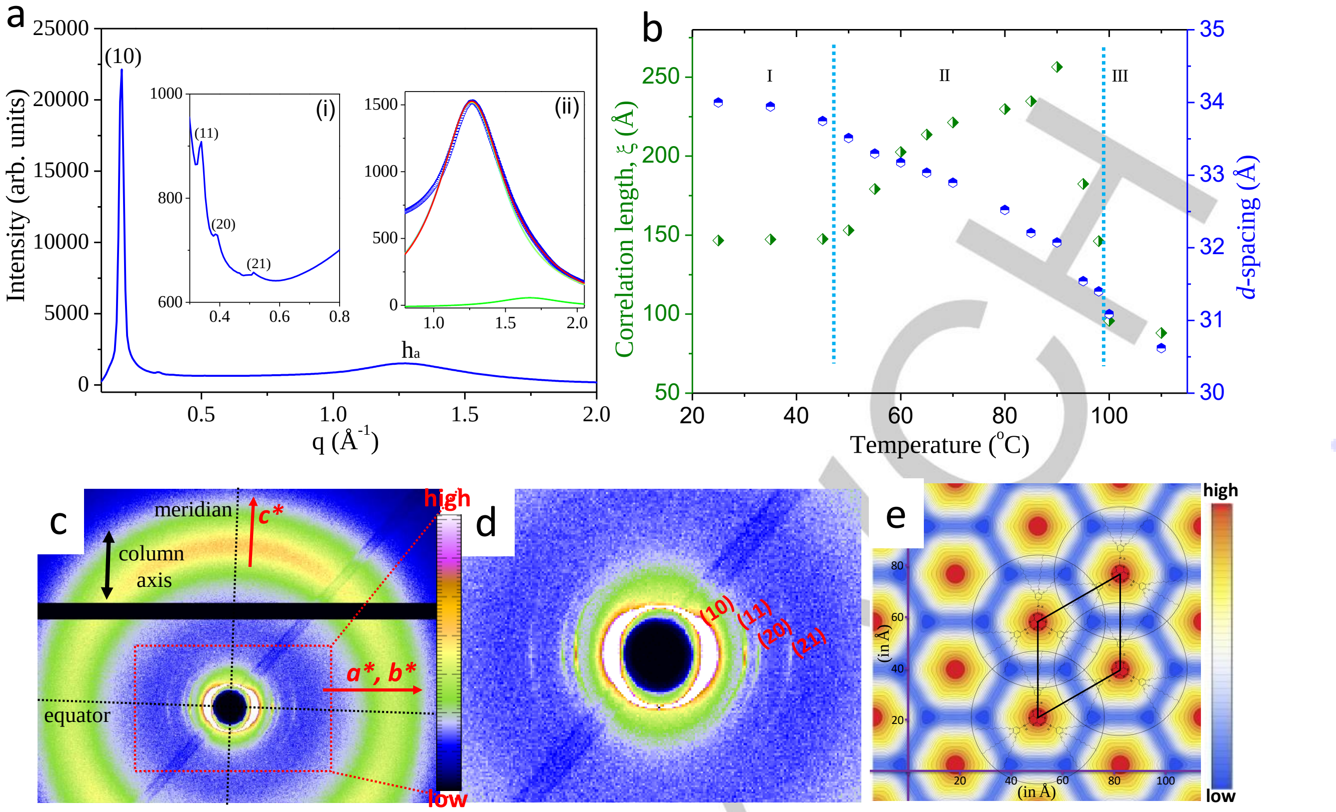

Figure 3. (a) X-ray diffraction pattern of col$_h$ phase of compound **3c** at 90 °C, Inset shows (i) zoomed area of small angle region in col$_h$ phase (ii) deconvolution of the wide angle peak at 90 °C, the curve with half-filled diamond in blue color represents the wide angle data. The curves in the cyan and green colors correspond to fluid chain-chain and heptazine core-core (face to face, h$_c$) correlations, respectively. And curve in the red color is the sum of the cyan and green color curve. h$_a$ - fluid chain-chain correlations, and h$_c$ – heptazine core-core (face to face) correlations (b) Variation of correlation length (ξ) and *d*-spacing corresponding to (10) peak with temperature for compound **3c** (c) Corresponding 2D aligned X- ray diffraction pattern of **3c** recorded at 90 °C; a*, b* and c* are the reciprocal lattice vectors (d) Zoomed area of small angle regime with indexing (b) Reconstructed electron density map of **3c** in Col$_h$ phase, showing the arrangement of the column on the 2D hexagonal lattice. Red represents the highest electron density and deep blue is the lowest. Parellelogram in black color on the map shows the respective 2D unit cell.

However, in the temperature range 25 °C to 45 °C, the higher order reflections ((11), (20) and (21)) are very weak and also the (10) peak is broader than that of at 90 °C (Fig. S14, ESI). Nonetheless, in the temperature range 45 °C to 98 °C, the higher orders reflections are developing and (10) peak gets sharper with increasing the temperature. Moreover, in the temperature range between 98 °C to 110 °C, the peak corresponding to (10) becomes broad and with no signature of hexagonal (Col$_h$) phase, confirming the appearance of isotropic phase. In-order to quantify the phase behavior, correlation length has been calculated. The variation of correlation length (ξ) and *d*-spacing corresponding to (10) peak (first small angle peak) with temperature is shown in the Fig. 3b. The *d*-spacing is found to be decrease continuously from 34.00 Å at 25 °C to 30.62 Å at 110 °C. However, the variation of correlation length (ξ) exhibit three clear regions: (I) 25 °C to 45 °C, (II) 45 °C to 98 °C and (III) 98 °C to 110 °C (Fig. 3b). The correlation length in the first region is about 146.6 ± 3.5 Å and remains same within this temperature range. However in the second regime, it is found to be increase rapidly from 153.0 ± 3.5 Å at 50 °C and reaches a maximum to 256.5 ± 3.5 Å at 90 °C and decreases to 146.2 ± 3.5 Å at 98 °C and then dropped quickly in the third region to 88.0 ± 3.5 Å at 110 °C. These regions, I, II and III are corresponded to Col$_h$ phase with most likely glassy in nature, Col$_h$ phase and isotropic liquid phase, respectively. The behavior of ξ with temperature could be understood as follows. As temperature increases alkyl chain becomes more fluid which results into better packing in Col$_h$ phase and hence ξ increases as observed in the second region. However, at very higher temperature the thermal vibration breaks the lattices and leads to isotropic liquid phase and thus ξ decreases as observed in the third region.

In brief, the compound **3b** exhibit Sm structure in the mesophase. The Sm structure most possibly could be induced by the hydrogen bonded ribbon like aggregation of the heptazine ring (Fig. 4a (i)). The schematic of the most plausible layer structure of Sm phase is shown in the Fig. 4a. In contrast to **3b**, **3c** showed Col$_h$ phase and further the X-ray diffraction results, electron density map and the calculated value of *n* (number of molecule per unit cell) allows the Col$_h$ phase to be schematically drawn as shown in the Fig. 4b. The observed Sm to Col$_h$ phase transformation with increasing peripheral chain length from **3b** to **3c** could be understood as follows. As peripheral chain length increases, alkyl chains become more flexible and as a result they cannot better accommodate in the Sm phase. Therefore, the hydrogen bonding breaks and inconsequence each molecule behaves as a disc which assembled themselves and leads to the formation of hexagonal phase. Hence, the generation of the Sm and Col$_h$ phase is attributed to the formation of hydrogen-bonded ribbon and disc-like (with no hydrogen bonding) self-assembled structures. Further, this type of lamellar (Sm) to hexagonal transformation is also seen in some lyotropic systems.[17]

The photo-physical properties of compound **3b** and **3c** were carried out both in solution (chloroform as a solvent) as well as in solid state (Fig. S15, ESI). In solution state, compounds **3b** and **3c** show well resolved two peaks at 270 & 330 nm which are likely due to π-π* and *n*-π* transitions, respectively.[18] The emission spectra, however, exhibited one peak centered at 446 nm for **3b** and 487 nm for **3c** along with a shoulder peak at 412 nm. On the other hand, in the solid state, compounds **3b** and **3c** show their respective absorption peaks at 274 & 334 nm while the emission spectra showed a maxima centered at 475 nm for both the compounds (Fig. S15, ESI).

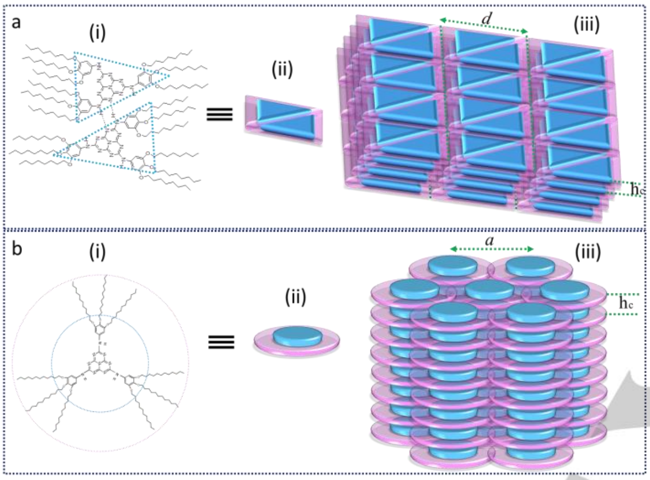

Figure 4. Plausible molecular packing model: (a) compound **3b** in Sm phase, (i and ii) Hydrogen-bonded ribbon-like aggregates of heptazine ring (iii) which assembled to form a layer structure of Sm phase (b) compound **3c** in Col$_h$ phase (i and ii) molecule modelled as a disc which amassed into column and (iii) form the columnar hexagonal structure.

Compound **3b** and **3c** were also found to be highly blue-light emissive (Fig. 5) (aggregation induced emission) in the solid state, while, in solution state the compound becomes non-emissive or weakly emissive (Fig. S16, ESI). The low band gap of 2 eV for compound **3c** is found as calculated from cyclic voltammetry (Fig. S17, ESI). In addition, conductivity measurement for compound **3c** was performed as detailed in ESI. The conductivity value obtained for the compound **3c** in the Col$_h$ are 1.12 x 10^{-7} Sm^{-1} (Fig. S18, ESI).

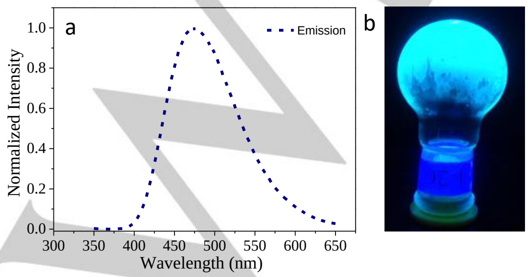

Figure 5. (a) Emission spectra of compound **3c** in the solid state (b) picture showing strong blue-light emission under UV light in the solid state for **3c**.

In summary, we present here the first report of heptazine based DLCs, possessing a stable Col$_h$ phase and a Sm phase at ambient temperature. They are strong blue light emitters when fabricated into solid thin films. Such materials with ease of synthesis, room temperature mesophase, solid state emitters along with low band gap are expected to be better candidates for future optoelectronic applications with the advantages that LCs offer.

Acknowledgements

SKP, IB and KK acknowledge CSIR, 02(0311)/17/EMR-II, CSIR-NET, DST-SERB (ECR/2016/001469), DST-Nano Mission (SR/NM/NT-06/2016) for financial support, respectively. We are grateful to NMR, HRMS and SAXS/WAXS facility at IISER Mohali.

Keywords: heptazine • room temperature • blue light • columnar hexagonal • smectic

[1] a) A. N. Cammidge , R. J. Bushby in *Handbook of Liquid Crystals*, *Vol. 7* (Eds. D. Demus, J. W. Goodby, G. W. Gray, H. W. Spiess, V. Vill), Wiley-WCH, Weinheim, **1998**, pp 693; b) R. J. Bushby, K. Kawata, *Liq. Cryst*. **2011**, *38*, 1415-1426; c) T. Wöhrle, I. Wurzbach, J. Kirres, A. Kostidou, N. Kapernaum, J. Litterscheidt, J. C. Haenle, P. Staffeld, A. Baro, F. Giesselmann, S. Laschat, *Chem. Rev.* **2016**, *116*, 1139-1241.

[2] a) S. Kumar, *Chem. Soc. Rev.* **2006**, *35*, 83-109; b) B. R. Kaafarani, *Chem. Mater.* **2010**, *23*, 378-396.

[3] a) S. Kumar, *Liq. Cryst.* **2004**, *31*, 1037-1059; b) S. Kumar, *Liq. Cryst.* **2005**, *32*, 1089-1113.

[4] S. Sergeyev, W. Pisula, Y. H. Geerts, *Chem. Soc. Rev*. **2007**, *36*, 1902-1929.

[5] a) S. Kumar, E. J. Wachtel, E. Keinan, *J. Org. Chem*. **1993**, *58*, 3821-3827; b) E. Keinan, S. Kumar, S. P. Singh, R. Ghirlando, E. J. Wachtel, *Liq. Cryst.* **1992**, *11*, 157-173.

[6] M. J. Sienkowska, J. M. Farrar, F. Zhang, S. Kusuma, P. A. Heiney, P. Kaszynski, *J. Mater. Chem.* **2007**, *17*, 1399-1411.

[7] R. Cristiano, J. Eccher, I. H. Bechtold, C. N. Tironi, A. A. Vieira, F. Molin, H. Gallardo, *Langmuir* **2012**, *28*, 11590-11598.

[8] F. Goettmann, A. Thomas, M. Antonietti, *Angew. Chem*. **2007**, *46*, 2717-2720.

[9] a) X. C. Wang, K. Maeda, A. Thomas, K. Takanabe, G. Xin, J. M. Carlsson, K. Domen, M. Antonietti, *Nat. Mat.* **2009**, *8*, 76-80; b) K. Kailasam, M. B. Mesch, L. Möhlmann, M. Baar, S. Blechert, M. Schwarze M. Schröder, R. Schomäcker, J. Senker, A. Thomas, *Energy Technol*. **2016**, *4*, 744-750.

[10] J. Li, H. Nomura, H. Miyazaki, C. Adachi, *Chem. Commun*. **2014**, *50*, 6174-6176.

[11] B. Jürgens, E. Irran, J. Senker, P. Kroll, H. Müller, W. Schnick, *J. Am. Chem. Soc*. **2003**, *125*,10288-10300.

[12] J. Li, T. Nakagawa, J. Macdonald, Q. Zhang, H. Nomura, H. Miyazaki, C. Adachi, *Adv. Mater*. **2013**, *25*, 3319-3323.

[13] R. S. Hosmane, M. A. Rossman, N. J. Leonard, *J. Am. Chem. Soc*. **1982**, *104*, 5497-5499.

[14] E. Kroke, M. Schwarz, E. Horath-Bordon, P. Kroll, B. Noll, A. D Norman, *New. J. Chem*. **2002**, *26*, 508-512.

[15] a) W. Zheng, N. B. Wong, W. Wang, G. Zhou, A. Tian, *J. Phys. Chem. A* **2004**, *108*, 97-106; b) H. K. Dambal, C. V. Yelamaggad, *Tetrahedron letters* **2012**, *53*, 186-190; c) K. C. Majumdar, N. De, B. Roy, A. Bhaumik, *Liq. Cryst.* **2010**, *37*, 1459-1464.

[16] a) E. Wuckert, M. Dix, S. Laschat, A. Baro, J. L. Schulte, C. Hägele, F. Giesselmann, *Liq. Cryst.* **2004**, *31*, 1305-1309; b) W. Li, J. Zhang, J. B. Li, M. Zhang, L. Wu, *Chem. Commun*. **2009**, 5269-5271.

[17] J. A. Schröter, C. Tschierske, M. Wittenberg, J. H. Wendorff, *J. Am. Chem. Soc*. **2006**, *120*, 10669-10675.

[18] D. R. Miller, D. C. Swenson, E. G. Gillan, *J. Am. Chem. Soc*. **2004**, *126*, 5372-5373.

Entry for the Table of Contents

Layout 1:

COMMUNICATION

Room temperature DLCs based on heptazine, a novel electron deficient and photolouminiscnt central core, are reported and their mesomorphic behavior investigated for the first time.

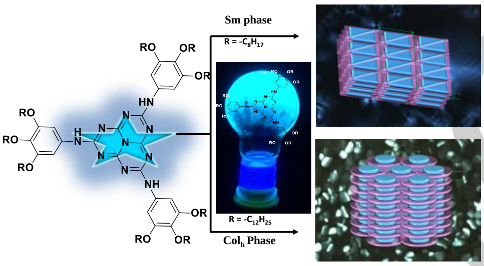

I. Bala, H. Singh, V. R. Battula, S. P. Gupta, J. De, S. Kumar, K. Kailasam* and S. K. Pal*

1-4

Heptazine: A new electron deficient fluorescent core for discotic liquid crystals